DOI: 10.23968/2500-0055-2024-9-3-39-52

EXPERIMENTAL INVESTIGATION ON THE SHEAR RESISTANCE OF I-SHAPED PERFORATED CONNECTORS IN COMPOSITE BEAMS

Farid Boursas*, Rafik Boufarh, Abderrahmani Sifeddine

Laboratory of Applied Civil Engineering (LGCA), Department of Civil Engineering,
Echahid Cheikh Larbi Tebessi University, Algeria

*Corresponding author's email: farid.boursas@univ-tebessa.dz

Abstract

Introduction: Steel-concrete composite girders have been widely used in bridges, with the stability of the interface being crucial. Shear connectors and reinforced concrete slabs play a key role as interfaces. Understanding the interaction between the composite beam and slab is essential for predicting the overall system response. It is necessary to optimize the connection between steel beams and reinforced concrete slabs in steel-concrete composite girders and facilitate their assembly and installation on-site, emphasizing their pivotal role in upholding the structural integrity of composite systems. The **purpose of the study** was to conduct an experimental investigation and a numerical simulation using the finite element method. During the study, the following **methods** were used: examining the behavior of IPE and IPN perforated shear connectors using push-out tests. The main objective was to analyze how the I-shaped perforated connector, concrete slab, steel beam, and rebar affect the measured slip between the steel beam and concrete slab. To achieve that, specimens with IPE80 or IPN80 shear connectors having circular or long cut holes containing 8 mm or 6 mm diameter steel bars were used to enhance the connector's resistance against uplift forces. The test setup follows Eurocode 4 guidelines, focusing on hole shape and anti-lift rebar diameter parameters. The predominant failure modes were mainly dictated by the crushing of the concrete slab. As a **result**, it was found that the hole geometry of IPE and IPN perforated shear connectors significantly impacts shear load capacity and ductility. The long cut hole shape in IPE and IPN perforated shear connectors exhibits superior ultimate load capacity but less interfacial slip compared to the circular hole. The IPE and IPN perforated shear connectors demonstrated satisfactory ductility for all tested hole shapes, and the 3D finite element models are consistent with the test results.

Keywords: composite beams, I-shaped perforated connectors, load-slip behavior, push-out test, ductility, finite element method.

Introduction

In the pursuit of practical solutions for steel-concrete connection challenges in composite constructions, various types of connectors have been explored to optimize connector quantity, strength, cost effectiveness, and ease of on-site assembly. While only a handful of types of connectors have been endorsed by Eurocode due to their reliability and ease of implementation for most structures (Maquoi et al., 2010), limitations in shear strength and fatigue under cyclic loads in composite bridges have led to the exploration of alternative connectors.

Several alternatives, such as welded angles with anti-lift rebars and perforated plates, have been proposed to address these concerns (Bujnak, 2007). Perforated plates were developed in Germany for the construction of the composite bridge of Caroni in Venezuela (Jarek, 2004). U- and I-shaped connectors were developed by Viest et al. (1951). In a previous work by Farid and Boutagouga (2021), I-shaped connectors showed promise in their ability to withstand shear forces and prevent vertical separation, as illustrated in Fig. 1. When oriented optimally, the I-shape demonstrated significantly higher shear strength than other orientations but exhibited minimal resistance to vertical separation.

This paper focuses on using perforated I-connectors with anti-lift rebars to enhance vertical separation resistance, improve the connector's ability to withstand shear forces, and prevent vertical separation between the steel beam and concrete slab. Unlike the U-connector, the perforated I-connector displays consistent behavior in both directions. It offers manufacturing ease through transverse cutting of IPN and IPE profiles, similar to the welding process for U-connectors.

Perforated shear connectors, known for their high bearing capacity and ductility, are increasingly favored in composite steel-concrete structures, especially when other connectors lack sufficient strength (Liu et al., 2021). Vianna et al. (2008) conducted an in-depth examination of perforated T-connectors, analyzing their performance in relation to concrete slab thickness, compressive

Fig. 1. IPE shear connectors studied in different orientations (Farid and Boutagouga, 2021)

strength, connector geometry, placement, and hole configuration. They also compared the outcomes of push-out tests with an analytical model proposed by different researchers in a comparative study between perforated plates and perforated T-connectors (Vianna et al., 2009). Another parametric study on perforated connectors demonstrated that increasing the number of holes in the connector increases its resistance. For each additional hole, there was an average increase in resistance of approximately 5 %. It was deduced that the concrete cylinders formed through the holes do not play a dominant role in strength compared to other factors such as plate bearing or slab reinforcement.

However, it is important to note that having at least one hole is crucial to ensure proper behavior and prevent undesired uplift. The study also revealed that the uplift remained controlled and consistent in magnitude for all perforated connectors (Cândido-Martins et al., 2010). Ahn et al. (2010) introduced a modified shear strength equation, considering perforated plates and rebar spacing based on push-out tests. Costa-Neves et al. (2013) explored eight new specimens featuring innovative geometries such as the I-Perfobond and the 2T-Perfobond, alongside an analytical model that accounted for connector geometry and reinforcing bars through holes. This included a comparison of experimental results with analytical models for perforated I- and T-shaped shear connectors.

A model developed by Su et al. (2014) overlooked the effects of specimen size and friction on the structural performance of the connector with a perforated plate. An analysis of the failure mechanism of perfobond rib shear connectors revealed a consistent occurrence of brittle failure in these connectors. Zheng et al. (2016) conducted a study with 21 push-out tests using circular and oblique hole perforated connectors, comparing these results against 10 shear resistance equations from the literature. Allahyari et al. (2018) used 90 literature records to develop a Bayesian neural network model that expresses the shear strength of perforated connectors with bars. Kim et al. (2018) examined the behavior of perforated Y-shaped shear connectors with double-row bars using push-out tests. Their investigation focused on exploring connector spacing, quantity, and three variations of single and double-row specimens. Zhao et al. (2018) conducted an experimental study involving 18 deeply anchored PBL shear connectors within reinforced concrete slabs. The findings highlighted that the hole diameter in the perforated steel plate, the diameter of reinforcing bars, and the transverse reinforcement ratio significantly influenced the bearing capacity. To address the challenges of installing reinforcements within circularly perforated connectors, Wang et al. (2018) proposed creating vertical sections in perforated plates to facilitate implementation and further study the behavior of this connector.

Methods

Composite constructions with steel and concrete have proven to outperform any other type of construction, particularly for main structures such as commercial buildings, residential buildings, and many bridges. They offer greater stiffness and strength to steel, as well as improved ductility.

This study explores the behavior of IPE and IPN perforated steel shear connectors, specifically those perforated with either circular or long cut holes, as depicted in Fig. 2. Experimental tests were conducted to analyze and compare these connector

types with regard to their shear strength, ductility, and failure modes.

Specimen preparation

The composite beams under investigation consisted of a HEB160 steel beam connected to a reinforced concrete slab with dimensions of 36 × 32 × 12 cm^3. The slab was reinforced with 4Φ8 reinforcements in two directions, as illustrated in Fig. 3. The connection between the steel beam and the concrete slab involves either IPE80 or IPN80 profile perforated shear connectors placed within circular and long cut holes with diameters of 6 and 8 mm, respectively, passing through the perforations.

All selected specimens adhered to the standard dimensions outlined in Eurocode 4 (2006) specifications (Fig. 4). This study used conventional concrete for the concrete slab material.

Material properties

Steel

Steel coupons were cut from the IPE80 and IPN80 webs and underwent standard coupon tensile testing to establish the stress-strain curve of the connectors. The specimen dimensions aligned with those typical for tensile tests on metallic materials (Aegerter et al., 2011). From these tests, crucial material properties such as yield strength and ultimate tensile stress of the connectors were determined and are detailed in Table 1.

Table 1. **Mechanical properties of the connector**

Type	f_y (MPa)	f_u (MPa)
IPE80	238	358
IPN80	247	385

Fig. 2. IPE and IPN perforated shear connectors under study

Fig. 3. Push-out specimen preparation

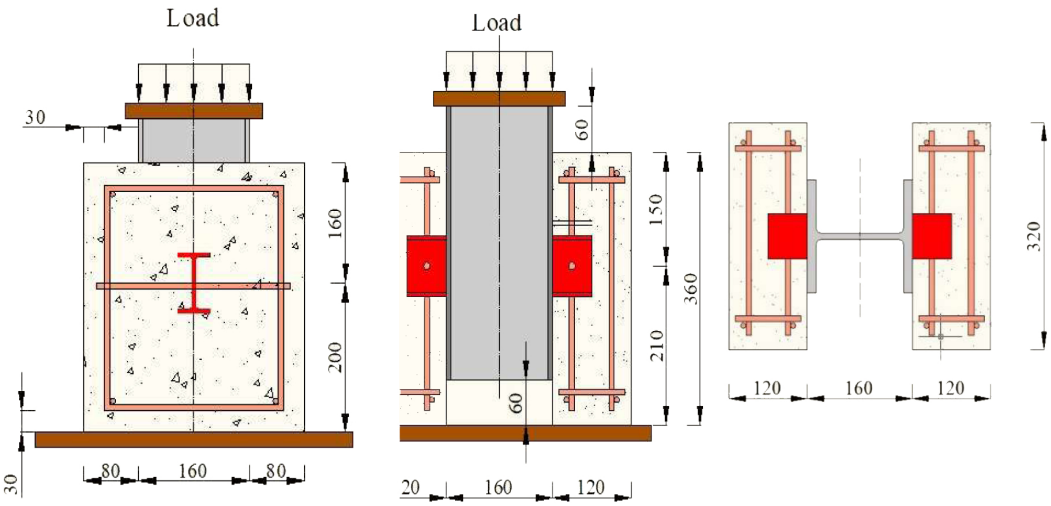

Fig. 4. Specimen dimensions (mm)

Concrete

The concrete mixture proportions for the slab were determined using the Dreux-Gorisse method (Dreux and Festa, 2007). All push-out specimen slabs were horizontally cast following Eurocode 4 standards, ensuring the elimination of friction at the steel-concrete interface by oiling the HEB flanges before casting the slab.

During the concrete casting process, three cylinders of concrete measuring 160 mm in diameter and 320 mm in length were formed from the same concrete mixture. These cylinders underwent compressive strength testing on the same day as the push-out tests were performed. The results of the tests are detailed in Table 2.

Table 2. **Compressive strength of concrete**

F_{c28} (MPa)	Average F_{c28} (MPa)
30.453	30.454
30.289	
29.866	
31.208	

Test setup and loading procedure

A concentrated monotonic load was applied to the top section of the HEB160 in the push-out specimens, as illustrated in Fig. 5. This load was applied using a calibrated hydraulic jack connected to an electric pump with a capacity of 500 kN. To measure the relative displacement between the HEB160 and the concrete slab, a linear variable differential transformer (LVDT) linked to a data acquisition system was placed at the top center of the HEB160. Two rigid steel plates, each 20 mm thick, were used to distribute the load uniformly. One was placed between the HEB160 and the hydraulic jack to spread the load across the entire HEB160 cross-section, while the other was positioned beneath the concrete slabs to provide a firm base. The test procedure adhered to Eurocode 4 (2006) standards. The load was initially applied incrementally in steps of 10 kN, ranging from 0 to 80 kN (equivalent to 40 % of the expected failure load), and then reduced to 10 kN (5 % of the expected failure load). Following this, a loading cycle between 10 and 80 kN was repeated 25 times to eliminate any inconsistencies in the test setup. The load was then continuously increased until failure occurred.

Results

The push-out tests investigated how IPE and IPN perforated shear connectors behave in composite girders. The main goal of this study was to analyze the load-slip behavior, ultimate shear capacity, and failure modes of the I-shaped perforated connectors.

I-shaped perforated connectors with a circular hole

The behavior of IPE and IPN perforated shear connectors with circular holes was examined during the initial experimental tests. The specimens under study were labeled as follows: IPE6C and IPN6C, denoting those with a 6 mm diameter of anti-lift rebar, while IPE8C and IPN8C represented specimens with an 8 mm diameter of anti-lift rebar (Fig. 5). Additionally, Fig. 6 illustrates the load-slip characteristics of these tested IPE and IPN perforated connectors featuring circular holes.

The findings indicate that IPE and IPN perforated connectors exhibit similar behavior, as illustrated in Figs. 6 and 7. Notably, IPE perforated connectors demonstrate marginally higher strength and ductility than their IPN counterparts. All specimens displayed remarkable ductility, meeting the 6 mm slip ductility limit. Failures occurred at slip measurements of 13.12 mm and 15.80 mm for IPE6C and IPE8C, and 12.98 mm and 12.58 mm for IPN6C and IPN8C, respectively. The diameter of the anti-lift rebar significantly impacts shear resistance, as evidenced

Fig. 5. Testing procedure

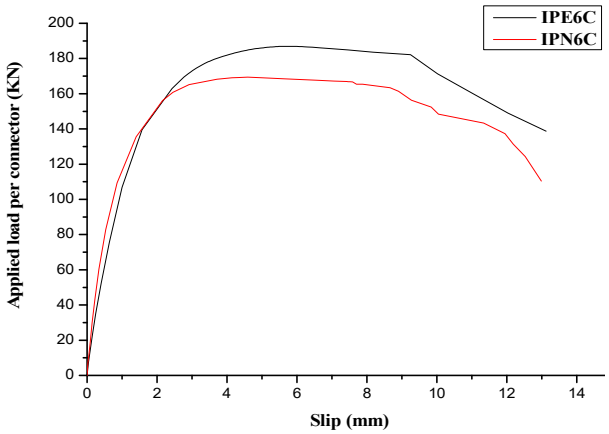

Fig. 6. Load-slip curves for IPE80 and IPN80 connectors with 6 mm rebar and a circular hole

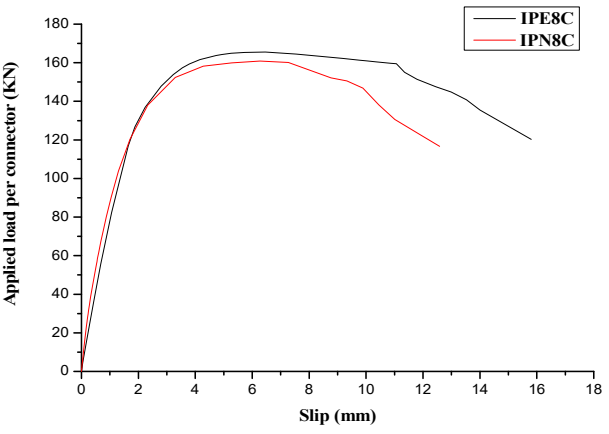

Fig. 7. Load-slip curves for IPE80 and IPN80 connectors with 8 mm rebar and a circular hole

by a decrease in load capacity with increasing rebar diameter in perforated connectors. Specifically, IPE6C and IPE8C failed at maximum loads of 186.92 kN and 165.52 kN per shear connector, while IPN6C and IPN8C failed at 169.39 kN and 160.90 kN per shear connector, respectively. Initial cracks appeared on the outer surfaces of the concrete slabs at a load of 115 kN per shear connector.

The initial cracks did not propagate deeply within the concrete slabs due to a 6 mm diameter anti-lift rebar. In IPE6C and IPN6C specimens, the anti-lift rebar effectively delayed the failure of the concrete slab. However, using an 8 mm diameter anti-lift rebar led to brittle concrete failure, accelerating crack propagation. In all cases of perforated connectors with a circular hole, the failure mode stemmed from concrete cracking and crushing, as seen in Fig. 8.

I-shaped perforated connectors with a long cut hole

Subsequent experimental tests examined the behavior of IPE and IPN perforated shear connectors featuring a long cut hole. This investigation explored how the hole shape impacts shear capacity, failure modes, and load-slip behavior. The specimens under scrutiny were labeled as follows: IPE6N and IPN6N, denoting those with a 6 mm diameter of anti-lift rebar, while IPE8N and IPN8N represented specimens with an 8 mm diameter of anti-lift rebar.

As shown in Figs. 9 and 10, IPE6N and IPE8N connectors exhibited ultimate shear capacities of 192.65 kN and 170.70 kN per connector, with ultimate slip capacities of 13.26 mm and 16.72 mm, respectively. Conversely, for IPN6N and IPN8N, the ultimate shear capacities were 172.30 kN and 168.89 kN per connector, with ultimate slip capacities of 12.68 mm and 10.81 mm, respectively. All the examined specimens notably exhibited reasonably robust ductile behavior.

The failure mode in all specimens of the perforated connectors with a long cut hole was due to concrete cracking and crushing. The early cracks observed on the surface of the concrete slabs started around the connector located in the middle of the slab at a load of approx. 155 kN per connector. The cracks are due to perforated rebar and the strength of the concrete slab, as shown in Fig. 11.

Analytical bearing capacity of I-shaped perforated connectors

Several analytical models have been proposed to estimate the bearing capacity of perforated connectors. Zheng et al. (2016) classified the equations proposed in the literature into three categories: the first is based on the resistance of the steel bar passed through the hole, the second is based on the strength of the reinforced concrete slab, and the third is based on the shape and distribution of the holes. Leonhardt et al. (1989) proposed the first analytical model with a simple

Fig. 8. Failure of IPE6C, IPE8C, IPN6C and IPN8C specimens

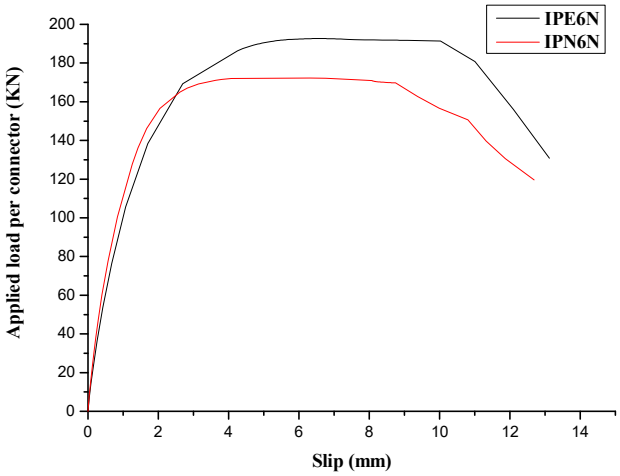

Fig. 9. Load-slip curves for IPE80 and IPN80 connectors with 6 mm rebar and a long cut hole

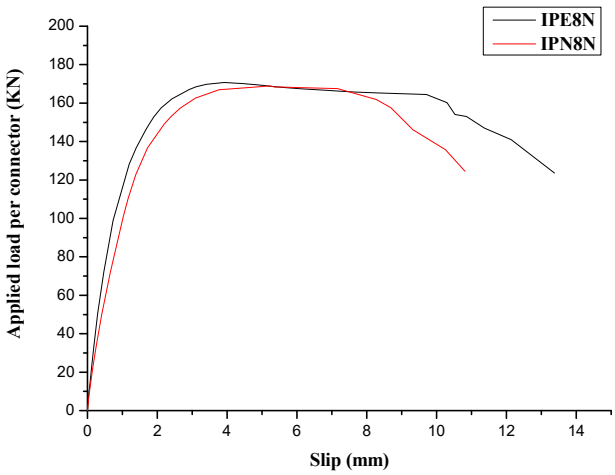

Fig. 10. Load-slip curves for IPE80 and IPN80 connectors with 8 mm rebar and a long cut hole

Fig. 11. Load-slip curve for IPE80 and IPN80 connectors with 8 mm rebar and a long cut hole

equation that only considers the resistance of the concrete slab, as shown in Table 3. Oguejiofor and Hosain (1994) proposed a more elaborate equation that considered the slab and connector resistances by considering the concrete strength and section, as well as the steel connector strength and section. Medberry and Shahrooz (2002) adjusted the coefficients of the equation proposed by Oguejiofor and Hosain (1994). They considered the details of the geometry of the connector, such as the height and width of the perforated connectors. Veríssimo et al. (2006) derived a modified equation to evaluate

the shear capacity of perforated connectors, based on the work of Oguejiofor and Hosain (1994). This modified equation was proposed based on the results of push-out tests and statistical analysis. Al-Darzi et al. (2007) proposed an analytical model that estimates the shear capacity of the perforated connector based on the results of a parametric study they conducted using a finite element-based model of push-out tests.

Additionally, the equation for estimating the bearing capacity must consider not only the steel bar passing through the cut hole, but also the shape of the push-out specimen, the geometry of the cut connector, and the properties of the materials used (Ahn et al., 2010). Zhao and Liu (2012) proposed an equation that considers the anchoring of the concrete in the hole, the contribution of the reinforcement passing through the hole, and the effect of the confinement on the strength of the concrete. Zheng et al. (2016) proposed a model to estimate the shear capacity of circular and long-cut hole perforated connectors. To adapt the model to different hole geometries, they proposed replacing the d^2 and d_s^2 variables in Eq. 7 with $4A/\pi$ and $4A_s/\pi$, respectively, as shown in Table 3.

An estimate of the load-bearing capacity of IPE80 and IPN80 perforated shear connectors was made based on the analytical models proposed in the literature. The obtained results are listed in Table 4.

As shown in Table 4, the shear capacity of perforated connectors obtained from the analytical models provided in the literature is very dispersed and cannot effectively predict the shear capacity of IPE and IPN perforated connectors. The closest models are those by Leonhardt and Veríssimo, as shown in Table 5. Based on analytical equations analysis, none of the equations account for all parameters affecting shear strength simultaneously. New equations must be developed to consider the geometry and resistance of the concrete slab, as well as the transverse reinforcement. This should also include all dimensions of the perforated plate, such as length, height, and thickness, along with the mechanical characteristics of the material used. Finally, the area of the perforated section and the

Table 3. **Analytical models for the bearing capacity of perforated connectors**

Authors	Equations	
Leonhardt et al. (1989)	$V_u = 2,23\ Af_c$	(1)
Oguejiofor and Hosain (1994)	$V_u = 4,5h_{sc}t_{sc}f_c + 0,91\ A_{tr}f_y + 3,31\mathrm{n}d^2\sqrt{f_c}$	(2)
Medberry and Shahrooz (2002)	$V_u = 1,66\mathrm{nA}\sqrt{f_c} + 0,9\ A_{tr}f_y + 0,747\mathrm{b}h_{ecs}\sqrt{f_c} + 0,413b_f L_c$	(3)
Veríssimo et al. (2006)	$V_u = 31,85.10^6\left(\frac{A_{tr}}{A_{cc}}\right) + 0,16\ A_{cc}\sqrt{f_c} + 4,04\left(\frac{\mathrm{h}}{\mathrm{b}}\right)\mathrm{ht}f_c + 2,37\mathrm{n}d^2\sqrt{f_c}$	(4)
Al-Darzi et al. (2007)	$V_u = 2,53.10^{-10}\,\mathrm{A}\sqrt{f_c} - 7,59.10^{-10}\ A_{tr}f_y + 7,62.10^{-4}\,\mathrm{ht}f_c + 255,310$	(5)
Ahn et al. (2010)	$V_u = 3,14\mathrm{ht}f_c + 1,21A_{tr}f_y + 2,98\mathrm{n}d^2\sqrt{f_c}$	(6)
Zhao and Liu (2012)	$V_u = 1,38\left(d^2 - d_s^2\right)f_c + 1,24d_s^2 f_y$	(7)
Zheng et al. (2016)	$V_u = 1,76(3,8(\frac{A_s}{\mathrm{A}})^{\frac{2}{3}}\left(\mathrm{A} - A_s\right)f_c + 1,58A_s f_y$	(8)

Table 4. **Analytical models for the bearing capacity of perforated connectors**

Hole shape	Specimens	Analytical shear load capacity (kN)							
		1	2	3	4	5	6	7	8
Circular	IPE6C	195.89	114.01	223.84	174.94	259.76	137.57	241.26	257.26
	IPN6C	166.54	114.57	223.74	178.32	259.85	137.96	241.26	257.26
	IPE8C	195.89	114.01	223.84	174.94	259.76	137.57	406.96	424.94
	IPN8C	166.54	114.57	223.74	178.32	259.85	137.96	406.96	424.94
Long cut	IPE6N	195.89	121.87	225.61	180.57	262.05	144.64	389.45	295.89
	IPN6N	166.54	122.42	225.51	183.94	262.14	145.03	389.45	295.89
	IPE8N	195.89	121.87	225.61	180.57	262.05	144.64	517.14	494.29
	IPN8N	166.54	122.42	225.51	183.94	262.14	145.03	517.14	494.29

Table 5. **Comparison between the calculated shear resistance and experimental results of IPE and IPN perforated connectors**

Hole shape	Specimens	Ultimate shear load using the equations (kN)				
		Leonhardt et al. (1987)	Exp/Eq	Veríssimo et al. (2006)	Exp/Eq	Experimental ultimate shear load
Circular	IPE6C	195.89	0.95	174.94	1.07	186.92
	IPN6C	166.54	1.02	178.32	0.95	169.39
	IPE8C	195.89	0.84	174.94	0.95	165.52
	IPN8C	166.54	0.97	178.32	0.90	160.90
Long cut	IPE6N	195.89	0.98	180.57	1.07	192.65
	IPN6N	166.54	1.03	183.94	0.94	172.30
	IPE8N	195.89	0.87	180.57	0.95	170.70
	IPN8N	166.54	1.01	183.94	0.92	168.89

dimensions and resistance of the rebar passing through the holes should be considered.

Numerical modeling of push-out tests

To verify the experimental findings, a 3D finite element model for the IPE and IPN perforated shear connectors in push-out tests was developed using ABAQUS software (Fig. 12). Due to the symmetry, only half of the push-out test specimens was modeled. The three-dimensional C3D8R eight-node solid brick elements with reduced integration were used to mesh the concrete slab, the steel beam, the IPE80 and IPN80 perforated shear connectors, and the anti-lift rebar. The T3D2 two-node mesh element was used for rebar. The advantage of using a truss element is that the perfect bond can easily be defined by embedding the steel bars in a host region, such as a concrete slab in our case. The rigid base was modeled using the R3D4 discrete rigid element.

Figs. 13–14 depicts the non-linear stress-strain characteristics of concrete and I-connectors under compression and tension. The Concrete Damage Plasticity model from a material library (Barbero, 2023) was employed. The material dilation angle was set to 31, and an eccentricity value of 0.1 was used. Additionally, a ratio of 1.16 between biaxial compressive strength and uniaxial compressive strength was adopted, while the tensile-to-compressive meridian ratio was established as 0.667.

The contact pair method defines the “surface-to-surface” contact between the concrete slab, IPE80 and IPN80 perforated shear connectors, and rebar. In experimental push-out tests, the surface of the rigid base in contact with the concrete slab is generally greased to reduce friction. In our finite element model, frictionless contact interaction was

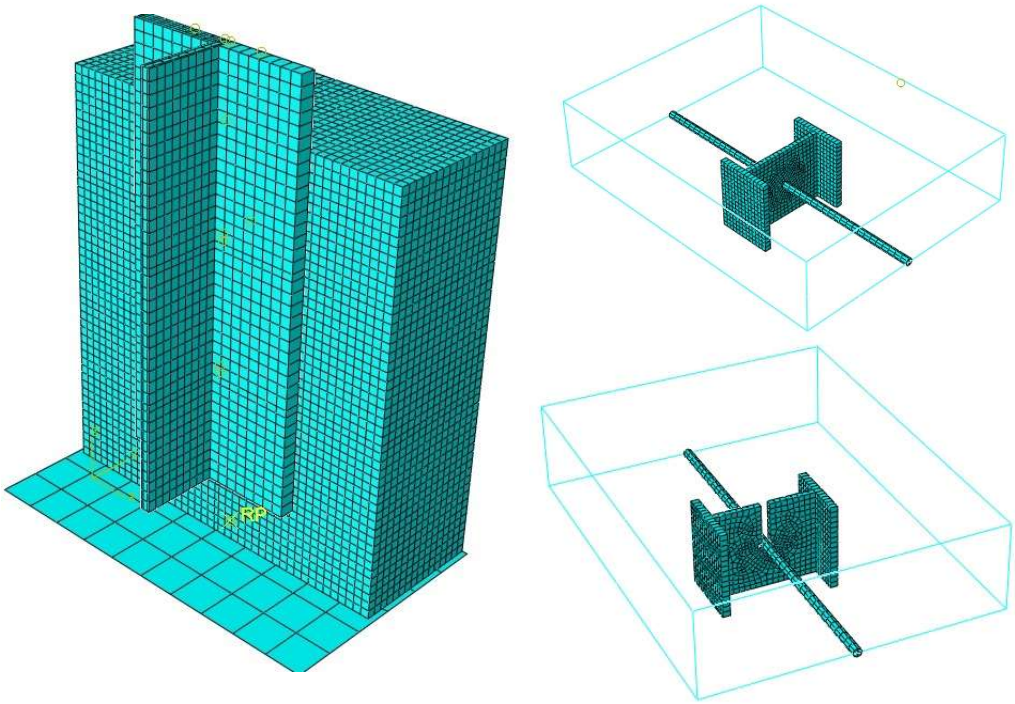

Fig. 12. Finite element mesh of the specimen

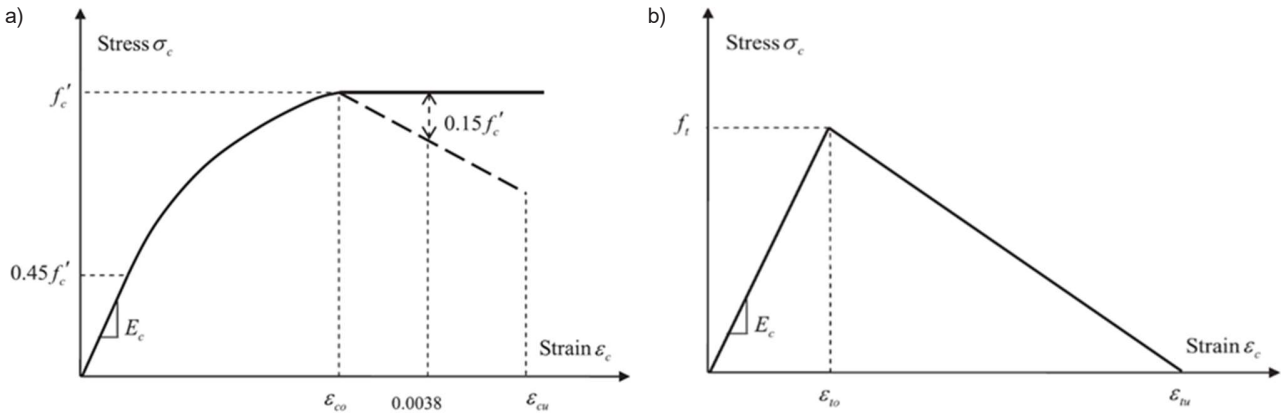

Fig. 13. Stress-strain relationship for concrete according to Eurocode 2 (1992): (a) compression, (b) tension

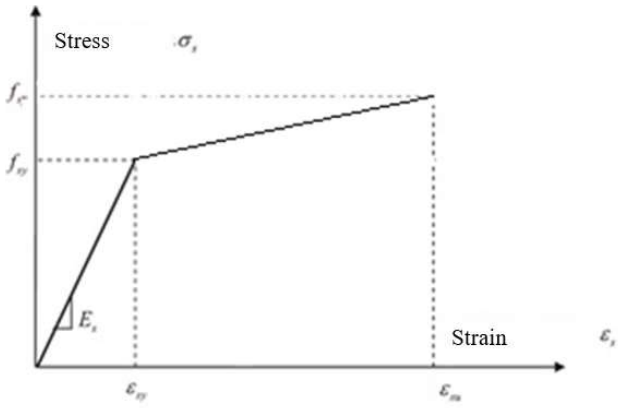

Fig. 14. Stress-strain relationship for I-connectors and reinforcement steel according to Eurocode 3 (1993)

applied to the surfaces of the rigid base and concrete slab. A tangential interaction was used for the interface between the I-shaped connector and the reinforced concrete slab, with a coefficient of friction set at 0.20. Reinforcing bars were located inside the concrete slab, as shown in Fig. 15. Integrated stress (embedded constraint) was applied to the rebar and slab.

The degrees of freedom of the rigid base reference node are all constrained. In this analysis, an imposed displacement is applied to the lower surface of the IPE80 and IPN80 perforated shear connectors, as shown in Fig. 16.

The numerical results obtained were compared with the results of the experimental tests.

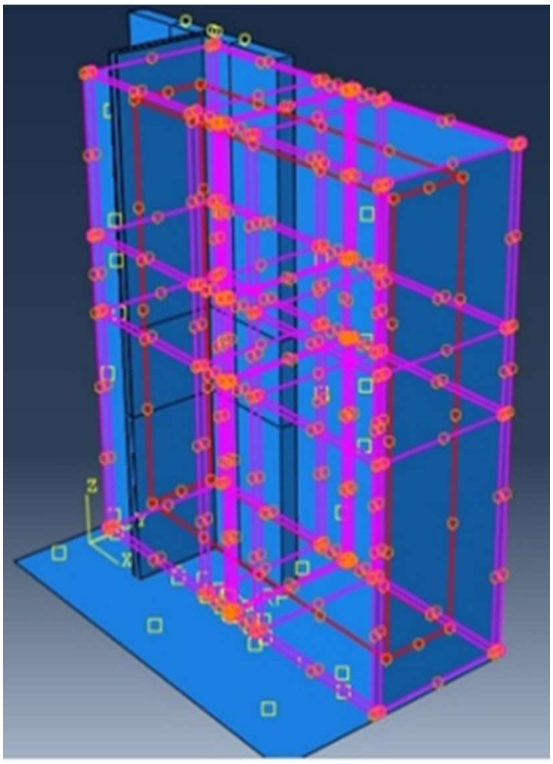

Fig. 15. Interaction and constraint conditions of the specimen

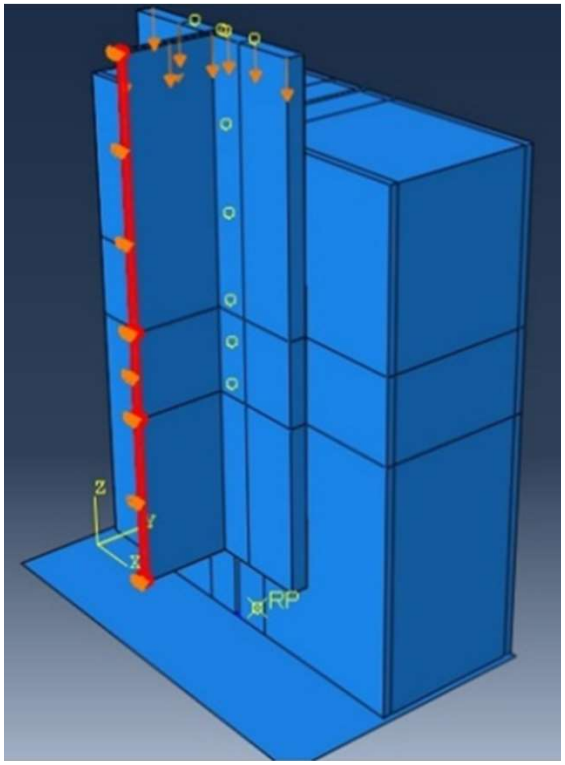

Fig. 16. Loading of the specimen

The comparison in the figures shows that the 3D finite element model established during this study can effectively predict the push-out strength and load-slip curve for push-out tests with perforated IPE80 and IPN80 connectors.

Figs. 17-20 compare the load–slip curves of the specimens with IPE and IPN perforated shear connectors obtained from the experiments with those predicted by the proposed finite element analysis. The results show good agreement between the experimental data and the finite element analysis. However, after reaching the ultimate load, the numerical curves diverge from the experimental curves. This discrepancy is attributed to differences in concrete mix standards across countries and the concrete material modeling used in the finite element analysis.

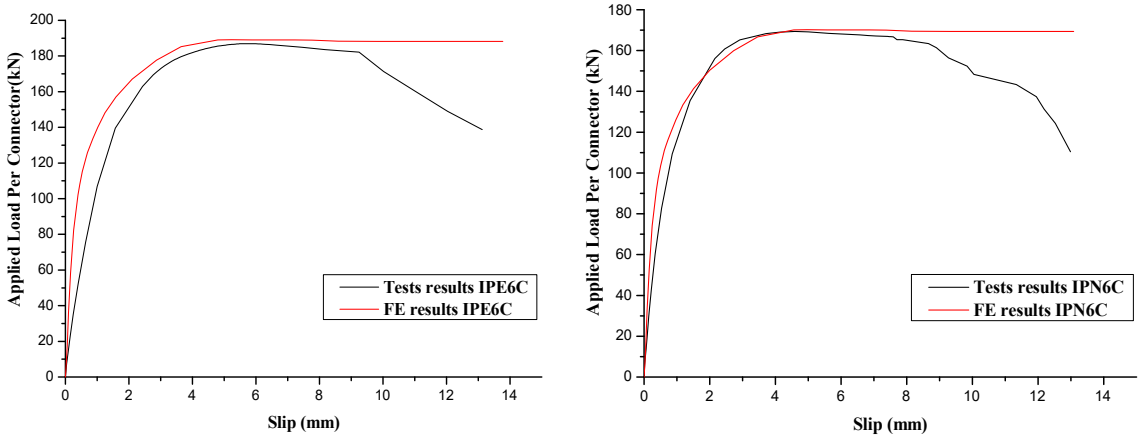

Fig. 17. Comparison of test and FE results for IPE80 and IPN80 connectors with 6 mm rebar and a circular hole

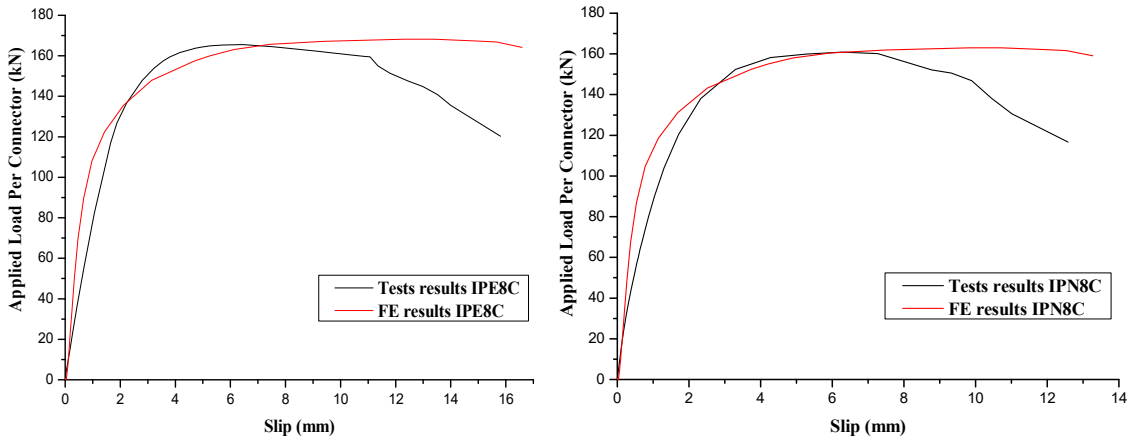

Fig. 18. Comparison of test and FE results for IPE80 and IPN80 connectors with 8 mm rebar and a circular hole

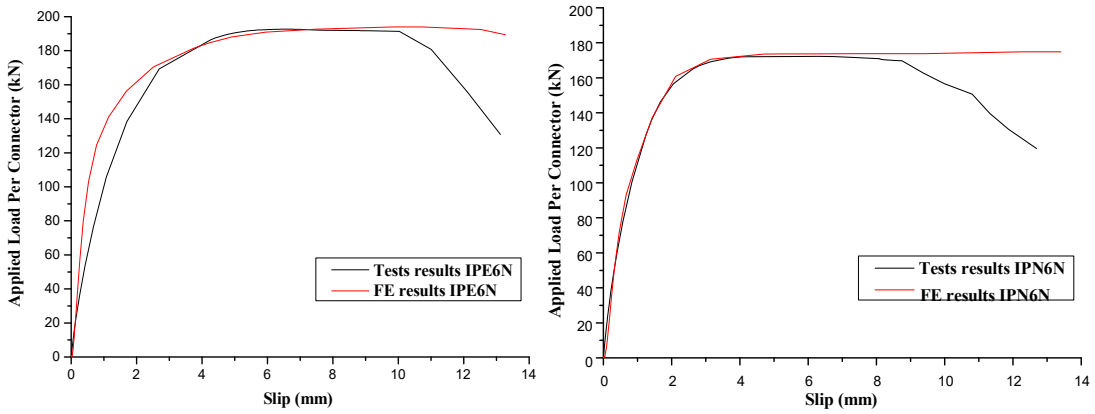

Fig. 19. Comparison of test and FE results for IPE80 and IPN80 connectors with 6 mm rebar and long cut hole

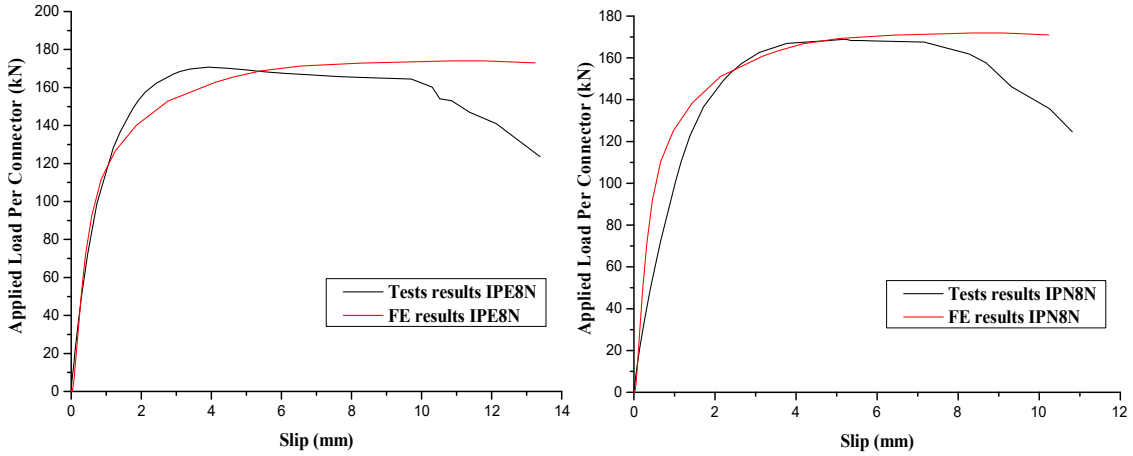

Fig. 20. Comparison of test and FE results for IPE80 and IPN80 connectors with 8 mm rebar and long cut hole

Conclusions

Eight push-out tests were conducted to examine the shear strength, ductility, and stiffness of IPE and IPN perforated shear connections in composite slabs. Based on the experimental results, several conclusions can be drawn:

- The geometry of the holes in IPE and IPN perforated shear connectors significantly impacts the shear load capacity and ductility.
- The long cut hole shape in IPE and IPN perforated shear connectors, which is more easily executed on-site, exhibits superior ultimate load capacity but less interfacial slip compared to the circular hole.
- The shear strength of IPE perforated connectors is comparable to that of IPN perforated connectors, with a slight advantage observed for IPE perforated connectors.
- IPE and IPN perforated shear connectors demonstrate satisfactory ductility across tested hole shapes.
- Increasing the diameter of the passing rebar from 6 mm to 8 mm for IPE connectors results in a 12 % decrease in load capacity but a 25 % gain in ductility. On the other hand, for IPN connectors, the load capacity decreases by approx. 5 % when the perforating rebar diameter increases from 6 mm to 8 mm for the hole types studied.
- The perforating rebar plays a crucial role, particularly in resisting uplift, meeting 10 % recommendation Eurocode 4, and contributing to shear resistance in the composite slab.
- The existing analytical equations for estimating the load capacity of perforated connectors do not consider all the parameters that simultaneously affect shear strength.
- The equations proposed by Leonhardt and Veríssimo are the closest to the experimental results for estimating the load capacity of IPE and IPN perforated shear connectors.
- The experimental results were compared with the outcomes of the finite element analysis, demonstrating good agreement for all push-out specimens. The mean difference in the ultimate shear resistance observed was 1.15 %.

Acknowledgments

This research was supported by Algeria's General Directorate for Scientific Research and Technological Development (DGRSDT). We would like to give special thanks to the University of Larbi Tébessi and the Laboratory of Applied Civil Engineering. Any opinions, findings, conclusions, or recommendations expressed in this publication are solely those of the authors.

References

1992. Eurocode 2: Design of concrete structures - Part 1-1: General rules and rules for buildings. BSI British Standards.

1993. Eurocode 3. Design of steel structures - Part 1-1: General rules and rules for buildings.. BSI British Standards.

1994. Eurocode 4: Design of composite steel and concrete structures - Part 1.1: General rules and rules for buildings. BSI British Standards.

Aegerter, J., Kühn, H.-J., Frenz, H., and Weißmüller, C. (2011). EN ISO 6892-1:2009 Tensile testing: initial experience from the practical implementation of the new standard*. *Materials Testing*, Vol. 53, Issue 10, pp. 595–603. DOI: 10.3139/120.110269.

Ahn, J.-H., Lee, C.-G., Won, J.-H., and Kim, S.-H. (2010). Shear resistance of the perfobond-rib shear connector depending on concrete strength and rib arrangement. *Journal of Constructional Steel Research*, Vol. 66, Issue 10**,** pp. 1295–1307. DOI: 10.1016/j.jcsr.2010.04.008.

Al-Darzi, S. Y. K., Chen, A. R., and Liu, Y. Q. (2007). Finite element simulation and parametric studies of perfobond rib connector. *American Journal of Applied Sciences*, Vol. 4, No. 3**,** pp. 122–127. DOI: 10.3844/ajassp.2007.122.127.

Allahyari, H., Nikbin, I. M., Saman Rahimi, R., and Heidarpour, A. (2018). A new approach to determine strength of Perfobond rib shear connector in steel-concrete composite structures by employing neural network. *Engineering Structures*, Vol. 157, pp. 235–249. DOI: 10.1016/j.engstruct.2017.12.007.

Barbero, E. J. (2023). *Finite Element Analysis of composite materials using Abaqus*. Boca Raton: CRC Press, 406 p.

Bujnak, J. (2007). *Analyse globale de poutres mixtes acier béton: approche analytique et modélisation non-linéaire.* DSc Thesis in Civil Engineering.

Cândido-Martins, J. P. S., Costa-Neves, L. F., and Vellasco, P. C. G. d. S. (2010). Experimental evaluation of the structural response of Perfobond shear connectors. *Engineering Structures*, Vol. 32, Issue 8**,** pp. 1976–1985. DOI: 10.1016/j.engstruct.2010.02.031.

Costa-Neves, L. F., Figueiredo, J. P., Vellasco, P. C. G. d. S., and Vianna, J. d. C. (2013). Perforated shear connectors on composite girders under monotonic loading: an experimental approach. *Engineering Structures*, Vol. 56, pp. 721–737. DOI: 10.1016/j.engstruct.2013.06.004.

Dreux, G. and Festa, J. (2007). *Nouveau guide de béton et ses constituants.* 8th edition. Paris: Eyrolles, 416 p.

Farid, B. and Boutagouga, D. (2021). Parametric study of I-shaped shear connectors with different orientations in push-out test. *Frattura Ed Integrità Strutturale*, Vol. 15, No. 57**,** pp. 24–39. DOI: 10.3221/igf-esis.57.03.

Jarek, B. (2004). *Fissuration de la dalle dans les poutres mixtes acier béton.* DSc Thesis.

Kim, S.-H., Han, O., Kim, K.-S., and Park, J.-S. (2018). Experimental behavior of double-row Y-type perfobond rib shear connectors. *Journal of Constructional Steel Research*, Vol. 150, pp. 221–229. DOI: 10.1016/j.jcsr.2018.08.012.

Leonhardt, F., Andra, W., Andra, H.-P., and Harre, W. (1989). New improved bonding means for composite load-bearing structures with high fatigue strength. *International Journal of Fatigue*, Vol. 11, No. 6**,** pp. 449–449. DOI: 10.1016/0142-1123(89)90207-7.

Liu, Y., Guo, L., Shi, J., and Wang, J. (2021). Push-out tests of shear connectors in U-shaped steel–concrete composite girder. *Structures*, Vol. 31, pp. 769–780. DOI: 10.1016/j.istruc.2021.02.018.

Maquoi, R., Debruyckere, R., Demonceau, J.-F., and Pyl, L. (2010). *Construction mixte*. Bruxelles: Infosteel8. Number of Pages 208.

Medberry, S. B. and Shahrooz, B. M. (2002). Perfobond shear connector for composite construction. *Engineering Journal*, Vol. 39, No. 1**,** pp. 2–12. DOI: 10.62913/engj.v39i1.771.

Oguejiofor, E. C. and Hosain, M. U. (1994). A parametric study of perfobond rib shear connectors. *Canadian Journal of Civil Engineering*, Vol. 21, No. 4**,** pp. 614–625. DOI: 10.1139/l94-063.

Su, Q.-T., Wang, W., Luan, H.-W., and Yang, G.-T. (2014). Experimental research on bearing mechanism of perfobond rib shear connectors. *Journal of Constructional Steel Research*, Vol. 95, pp. 22–31. DOI: 10.1016/j.jcsr.2013.11.020.

Veríssimo, G. S., Paes, J. L. R., Valente, I., Cruz, P. J. S., and Fakury, R. H. (2006). Design and experimental analysis of a new shear connector for steel and concrete composite structures. *In:* da Sousa Cruz, P. J., Frangopol, D. M., and Canhoto Neves, L. C. (eds.). *Advances in Bridge Maintenance, Safety Management, and Life-Cycle Performance.* London: CRC Press, pp. 1313–1322.

Vianna, J. d. C., Costa-Neves, L. F., Vellasco, P. C. G. d. S., and de Andrade, S. A. L. (2008). Structural behaviour of T-Perfobond shear connectors in composite girders: an experimental approach. *Engineering Structures*, Vol. 30, Issue 9**,** pp. 2381–2391. DOI: 10.1016/j.engstruct.2008.01.015.

Vianna, J. d. C., Costa-Neves, L. F., Vellasco, P. C. G. d. S., and de Andrade, S. A. L. (2009). Experimental assessment of Perfobond and T-Perfobond shear connectors' structural response. *Journal of Constructional Steel Research*, Vol. 65, Issue 2**,** pp. 408–421. DOI: 10.1016/j.jcsr.2008.02.011.

Viest, I. M., Siess, C. P., Appleton, J. H., and Newmark, N. M. (1951). Full-scale tests of channel shear connectors and composite t-beams. *University of Illinois Bulletin*, Vol. 50, No. 29**,** 155 p.

Wang, X., Liu, Y., and Liu, Y. (2018). Experimental study on shear behavior of notched long-hole perfobond connectors. *Advances in Structural Engineering*, Vol. 22, Issue 1**,** pp. 202–213. DOI: 10.1177/1369433218782991.

Zhao, C., Li, Z., Deng, K., and Wang, W. (2018). Experimental investigation on the bearing mechanism of Perfobond rib shear connectors. *Engineering Structures*, Vol. 159, pp. 172–184. DOI: 10.1016/j.engstruct.2017.12.047.

Zhao, C. and Liu, Y.-Q. (2012). Experimental study of shear capacity of perfobond connector. *Engineering Mechanics*, Vol. 29, No. 12**,** pp. 349–354. DOI: 10.6052/j.issn.1000-4750.2011.09.0604.

Zheng, S., Liu, Y., Yoda, T., and Lin, W. (2016). Parametric study on shear capacity of circular-hole and long-hole perfobond shear connector. *Journal of Constructional Steel Research*, Vol. 117, pp. 64–80. DOI: 10.1016/j.jcsr.2015.09.012.

ЭКСПЕРИМЕНТАЛЬНОЕ ИССЛЕДОВАНИЕ СОПРОТИВЛЕНИЯ СДВИГУ I-ОБРАЗНЫХ ПЕРФОРИРОВАННЫХ СОЕДИНИТЕЛЬНЫХ ЭЛЕМЕНТОВ В СОСТАВНЫХ БАЛКАХ

Фарид Бурса*, Рафик Буфар, Абдеррахмани Сифеддин

Университет Ларби Тебесси, Тебесса, Алжир

*E-mail: farid.boursas@univ-tebessa.dz

Аннотация

Введение: в сооружении мостов широко используются сталежелезобетонные составные балки, при этом решающее значение имеет стабильность стыка. Соединительные элементы, работающие на сдвиг, и железобетонные плиты играют ключевую роль в качестве соединителей. Для того чтобы спрогнозировать общую реакцию системы, необходимо понимание взаимодействия между составной балкой и плитой. Требуется оптимизировать соединение стальных балок и железобетонных плит в сталежелезобетонных составных балках и облегчить их сборку и установку на месте, акцентируя внимание на их ключевой роли в поддержании структурной целостности комбинированных систем. **Цель исследования** — выполнить экспериментальное исследование и численное моделирование с использованием метода конечных элементов. В ходе исследования использовались следующие **методы**: изучение поведения перфорированных соединительных элементов IPE и IPN, работающих на сдвиг, с помощью испытаний на выдавливание. Основной задачей было проанализировать, как I-образный перфорированный соединительный элемент, бетонная плита, стальная балка и арматура влияют на величину скольжения между стальной балкой и бетонной плитой. Для этого использовались образцы с соединительными элементами IPE80 или IPN80, работающими на сдвиг, с круглыми отверстиями и длинными отверстиями с прорезью, содержащими стальные стержни диаметром 6 и 8 мм, с тем чтобы повысить сопротивление соединительного элемента к воздействию сил отрыва. Испытательная установка соответствует рекомендациям Еврокода 4, при этом особое внимание уделяется форме отверстия и диаметру арматуры, работающей на сопротивление силам отрыва. Типы разрушения были главным образом обусловлены разрушением бетонной плиты. **Результаты**: было установлено, что геометрия отверстий в перфорированных соединительных элементах IPE и IPN, работающих на сдвиг, оказывает существенное влияние на пластичность и способность выдерживать сдвиговые нагрузки. Длинное отверстие с прорезью в перфорированных соединительных элементах IPE и IPN, работающих на сдвиг, обеспечивает более высокую предельную несущую способность, но меньшее скольжение между поверхностями по сравнению с круглым отверстием. Перфорированные соединительные элементы IPE и IPN, работающие на сдвиг, продемонстрировали удовлетворительную пластичность для всех рассмотренных форм отверстий, а трехмерные конечно-элементные модели согласуются с результатами испытаний.

Ключевые слова: составные балки, I-образные перфорированные соединительные элементы, сопротивление сдвигу в зависимости от нагрузки, испытание на выдавливание, пластичность, метод конечных элементов.